Hindawi
Journal of Nanomaterials
Volume 2019, Article ID 4184351, 8 pages
https://doi.org/10.1155/2019/4184351

Research Article

Characterization of Nanosilica/Low-Density Polyethylene Nanocomposite Materials

Malek Alghdeir, Khaled Mayya, and Mohamed Dib

Applied Physics Department, Higher Institute for Applied Sciences and Technology, Damascus, Syria

Correspondence should be addressed to Malek Alghdeir; malekghdeir@yahoo.com

Received 2 October 2018; Revised 22 November 2018; Accepted 19 December 2018; Published 20 March 2019

Guest Editor: Chandragiri V. Reddy

Six ratios of nanosilica particles were employed to fabricate low-density polyethylene (LDPE) composites using melt mixing and hot molding methods. Several composite films with different ratios (0.5, 1, 2.5, 5, 7.5, and 10 wt%) of SiO_2 were prepared. The obtained composite films were identified and characterized by Fourier-transform infrared spectroscopy (FTIR) and ultraviolet-visible spectroscopy (UV-VIS). At a specific mixing ratio, far infrared radiation transmittance was prohibited while the ultraviolet-visible transmittance is allowed; this will be explained in detail. Optical measurements show that the composite films prevent the transmission of IR radiation near 9 μm and allow UV-VIS transmission during sun-shining time. The mechanical behaviour of a nanosilica-reinforced LDPE composite was studied using tensile tests. The addition of 1 wt% nanosilica has successfully enhanced the mechanical properties of the LDPE material.

1. Introduction

Polymeric materials are widely used in food packaging and in greenhouses. Typical examples of such materials are polypropylene (PP), polyethylene (PE), and polyethylene terephthalate (PET) [1, 2].

During the past years, much effort has been devoted to polymer nanocomposites [3]. Polymer nanocomposites often show excellent mechanical properties compared to the traditional composites at a lower loading of the nanoparticles [4]. So far, a few researches have studied the effects of different nanoparticles on the performances of composite materials such as nanosilica [3]. The excellent performance of silica film has attracted attention in academia and industry due to its antiresistance, hardness, corrosion resistance [5], dielectric properties [6], optical transparency, etc. [7]. Silica as a thin film is widely used to improve the surface properties of materials. This is why silica thin films are used in many fields as in antireflection coating film field [8]. In the packaging industry, silica films are used as barrier layers in polymer packaging materials. Most of the modern packaging materials do not provide an efficient barrier against the permeation of gases. This leads to food and drinks getting rotten quickly. Because of this, a silica film deposited on the surface of the polymer packaging becomes popular and indispensable. Besides, silica films can be also used as corrosion protective layers of metals. Because of the universal application of silicon dioxide films in various fields, the preparation of silica with high quality is always an important aim of scientific research [9].

Lately, a number of different barrier technologies were being developed. Theoretically, a barrier function can be inserted into a plastic-based material via two different means: either by mixing a barrier material into the base polymer or by coating a layer of the barrier material on the polymer surface [10, 11].

The traditional method of preparing polymer/silica composites was direct mixing of the silica into the polymer. The mixing could be done by melt blending and solution blending. The main difficulty in the mixing process is the effective dispersion of the silica nanoparticles in the polymer matrix, because they usually tend to agglomerate [12].

This work represents the results of optical and thermal experiments on LDPE mixed with nanosilica particles at different ratios (0.5, 1, 2.5, 5, 7.5, and 10 wt%). The aim is to achieve a nanocomposite that prevents the transmittance

of IR radiation and allows the transmittance of UV-VIS, so that most of the thermal radiation of the ground and plants in the greenhouse is conserved. The mechanical properties of the nanocomposite, such as the tensile strength, the elongation at break, and Young's modulus, were also evaluated and discussed.

By studying the blackbody thermal radiation, all objects with a temperature above absolute zero were shown to emit energy in the form of electromagnetic radiation. A blackbody is a theoretical or model body which absorbs all radiation falling on it. It is a hypothetical object which is a "perfect" absorber and a "perfect" emitter of radiation. The electromagnetic radiation emitted by a blackbody has a specific spectrum and intensity that depends only on the body's temperature; the thermal radiation spontaneously emitted by ordinary objects, land, and plants, for example, can be approximated as blackbody radiation. Figure 1 shows the blackbody radiation spectrum at 273, 293, 313, 333, 373, 393, 413, 433, and 453 K. We are interested in the vicinity of 10 μm (9 to 11), because at the temperatures near 0°C, (273 K) the thermal radiation from the ground is the maximum at 10 μm, while at the temperature of 30°C (303 K), the thermal radiation from the ground is the maximum at 9.5 μm [9].

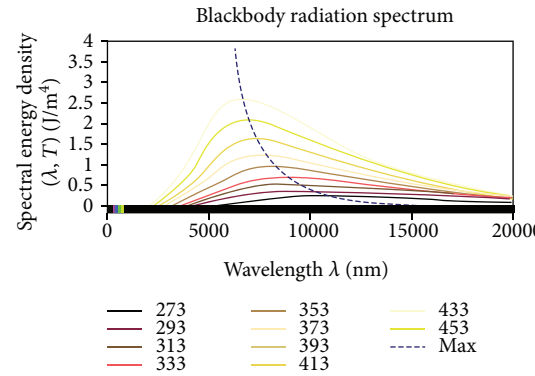

Figure 1: Blackbody radiation spectra at 273, 293, 313, 333, 373, 393, 413, 433, and 453 K. This figure was reproduced from Alghdeir et al. [9] (under the Creative Commons Attribution License/public domain).

2. Material and Methods

2.1. Materials. Low-density polyethylene (LDPE), a thermoplastic made from an ethylene monomer with a density of 0.922 g/cm^3, was purchased from Saudi Basic Industries Corporation (SABIC). High-purity fumed nanosilica (purity > 99%) with an average particle size of ~12 nm and the trademark of A200 was obtained from Evonik Degussa AG (Germany). Table 1 shows the basic physical and chemical properties of the fumed nanosilica used in the present work.

Table 1: Basic physical and chemical properties of fumed nanosilica.

Properties	Value
Physical state	Solid
Color	White
Form	Powder
pH	3.7-4.5
Surface area	200 ± 25 (m^2/g)
Melting point/range	Approx. 1700°C
Density	Approx. 2.2 g/cm^3
Water solubility	>1 mg/l
Thermal decomposition	>2000°C
Loss on drying	≤1.5% (2 hours at 105°C)
SiO_2 content based on ignited material	>99.8%

2.2. Sample Preparation. Samples were prepared by blending LDPE and silica with different ratios (0.5, 1, 2.5, 5, 7.5, and 10 wt%). The different nanosilica ratios were mechanically mixed with the LDPE granules at a processing temperature of 130°C and a speed of 50 rpm for 10 min using the internal mixer (Brabender Plasti-Corder PL-2200, W50, Germany). Films with dimensions of 10 cm × 10 cm × 120 μm of the neat LDPE and nanocomposites were obtained by a hot-press method at 140°C and under 50 bar. For the mechanical behaviour tests of the composite, other plates were prepared using the abovementioned procedure with a thickness of 1.8 ± 0.1 mm.

Table 2: Dimensions of samples for tensile test.

Specifications	Dimensions (mm)
Sample length	75
Display ends	12.5 ± 1
Length of the active part	25 ± 1
Display the effective part	4 ± 0.1
External radius	8 ± 0.5
Internal radius	12.5 ± 1

3. Results and Discussion

3.1. Study of Mechanical Properties. For the studies of mechanical properties, the test specimens were molded and cut according to the dimensions specified in Table 2.

The tensile test was achieved using a traction-compression machine (Adamel Lhomargy DY34) under atmospheric conditions. For each ratio, including the neat LDPE (the control sample), five samples were tested and their values were averaged. The tensile tests were carried at a speed of 5 mm/min. Table 3 shows a summary of the tensile data for the control sample and the samples of six composites.

Stress-strain curves from tensile tests for LDPE/silica nanocomposites are shown in Figure 2. It can be noticed that the stress at break gradually increases with the increase of up to 1 wt% of the silica ratio. This result suggests that the nanosilica particles would reinforce stress and cause the increase of the tensile strength of the nanocomposite.

Table 3: Summary of tensile data for the control sample and six composites of LDPE.

Material	Property	Sample no. 1	Sample no. 2	Sample no. 3	Sample no. 4	Sample no. 5	Average	Std. Dev.
Neat LDPE (control sample)	Maximum load (*N*)	60	60	50	60	60	58	4.47
	Tensile strength (MPa)	8.40	8.42	7.13	8.67	8.28	8.18	0.60
	% elongation at break	190	230	323	258	248	250	48
	Modulus of elasticity (MPa)	66.64	56.73	67.53	69.45	62.01	64.47	5.1
LDPE 0.5 wt% SiO_2	Maximum load (N)	60	60	60	60	60	60	0
	Tensile strength (MPa)	8.13	8.39	8.24	8.28	8.35	8.27	0.1
	% elongation at break	263	394	276	311	293	307	52
	Modulus of elasticity (MPa)	104	102	98	81	92	95.4	9.2
LDPE 1 wt% SiO_2	Maximum load (N)	60	60	60	60	60	60	0
	Tensile strength (MPa)	8.83	8.75	8.82	8.65	8.89	8.78	0.09
	% elongation at break	410	355	377	410	318	374	40
	Modulus of elasticity (MPa)	95	90	93	96	68	88.4	12
LDPE 2.5 wt% SiO_2	Maximum load (N)	60	60	60	60	60	60	0
	Tensile strength (MPa)	8.46	8.67	8.82	8.48	8.80	8.64	0.17
	% elongation at break	260	444	273	456	379	362	92
	Modulus of elasticity (MPa)	99	96	94	99	92	96	3.5
LDPE 5 wt% SiO_2	Maximum load (N)	60	60	60	60	60	60	0
	Tensile strength (MPa)	8.34	8.17	8.39	8.32	8.16	8.27	0.10
	% elongation at break	142	201	229	338	247	231	71
	Modulus of elasticity (MPa)	105	118	135	124	128	122	11
LDPE 7.5 wt% SiO_2	Maximum load (N)	60	60	60	60	60	60	0
	Tensile strength (MPa)	8.37	8.43	8.36	8.24	8.38	8.35	0.07
	% elongation at break	242	231	222	300	270	253	31
	Modulus of elasticity (MPa)	106	139	110	109	96	112	16
LDPE 10 wt% SiO_2	Maximum load (N)	60	60	60	60	60	60	0
	Tensile strength (MPa)	8.43	8.04	8.51	8.48	8.47	8.38	0.19
	% elongation at break	139	126	95	116	114	118	16
	Modulus of elasticity (MPa)	104	129	95	141	141	122	21

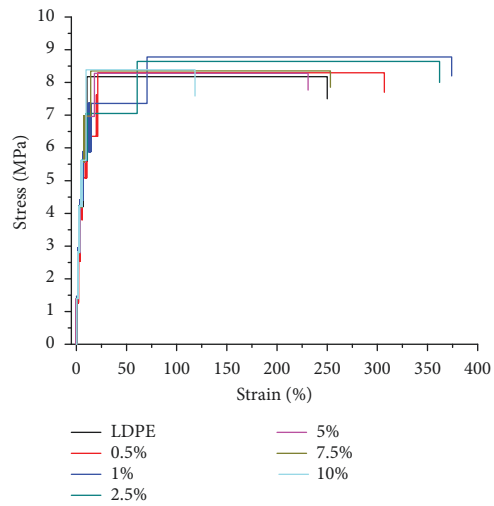

Figure 2: Typical stress-strain curves of neat LDPE and LDPE/silica nanocomposites.

Figure 2 also shows that the elongation at break values of the nanocomposite greatly increases with the nanosilica particle ratio that is also up to 1 wt%. This can be explained by the increase in the surface bonding between the molecules of the polymer, when the nanosilica particles are added to it. Similar results have been obtained with other oxides [13].

Beyond 1 wt%, it can be noticed from Figure 2 that the values of both the tensile strength and elongation at break of the nanocomposite decrease with the increase in the nanosilica particle ratio incorporated. This result can be explained by the agglomeration of the nanosilica particles within the polymer matrix. This agglomeration can even be seen with the naked eye in the form of white spots within the samples (see Figure 3).

Figure 4 shows the variations in Young's modulus of the nanocomposite with the nanosilica particle ratios. The elongation at break was also added to the figure. It can be noticed that Young's modulus increases with the nanosilica particle ratios of up to 5 wt%. Beyond this value, we notice that the values of Young's modulus remain practically

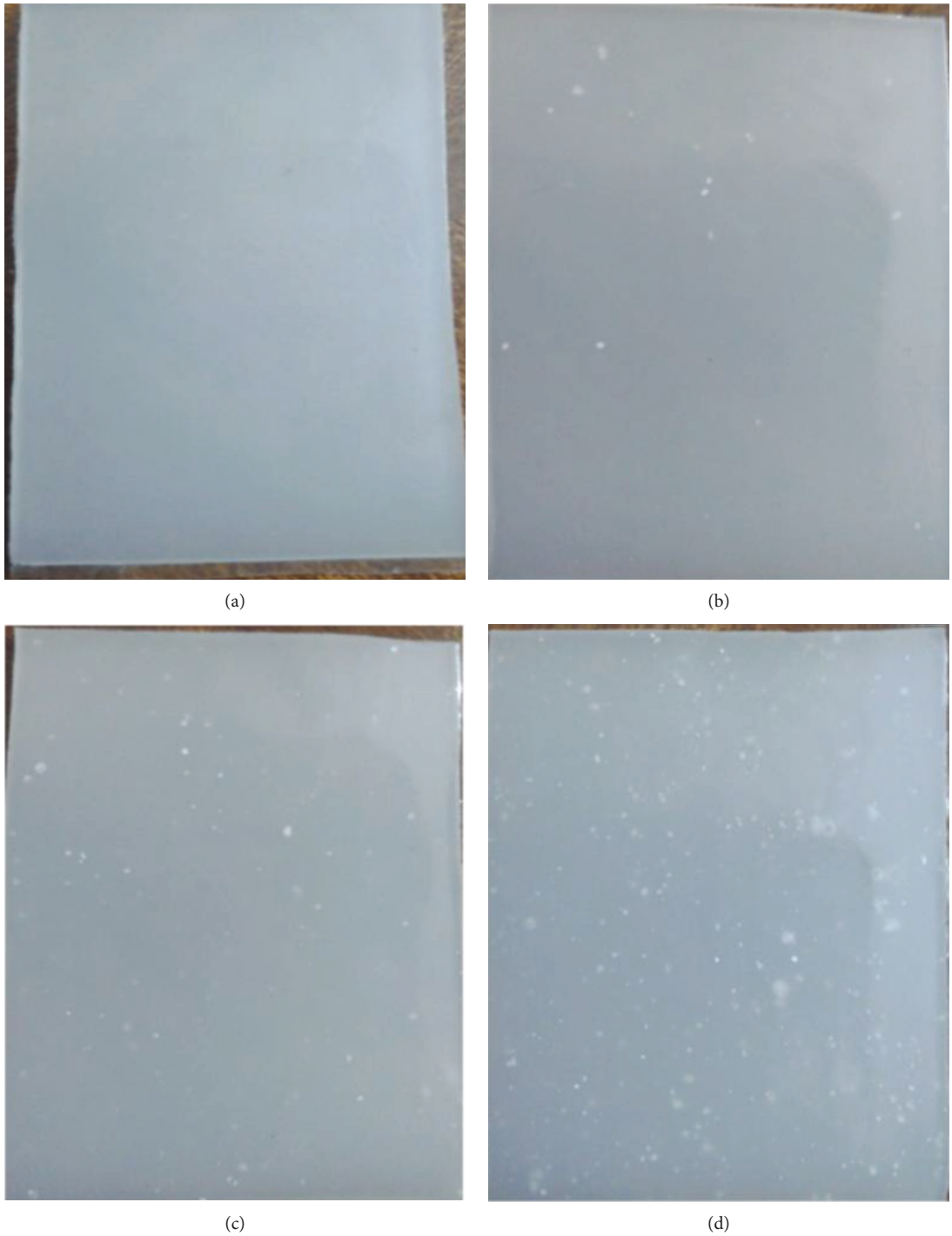

Figure 3: Images of the surface of the LDPE/silica composites containing (a) 0 wt%, (b) 1 wt%, (c) 5 wt%, and 10 wt% of nanosilica particles.

constant (up to the uncertainties). The already mentioned decrease in the elongation at break is explained by the agglomeration of the nanosilica particles within the polymer matrix, as already mentioned.

3.2. Optical Study

3.2.1. Infrared Spectroscopic Study. The transmittance of samples was examined by Fourier-transform infrared spectroscopy (FTIR) (VERTEX 70/70v FT-IR spectrometer from Bruker™ Optics) in the wavelength range of 1-25 μm. Figure 5 shows the transmittance spectra of the SiO_2/LDPE films with different ratios. Different absorption peaks could be identified in the MIR range. The first one at ~3 μm is caused by the OH group; other peaks at ~9 μm, ~12 μm, and ~21 μm are due to the Si-O-Si resonance mode of vibrations [14]. Some of these peaks also involve the LDPE substrate in the IR absorption spectra. The peak at 9 μm gives

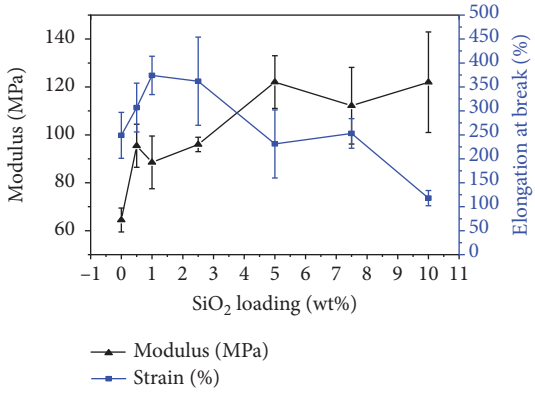

Figure 4: Elongation at break and modulus of elasticity (averaged values) as a function of different ratios of SiO_2.

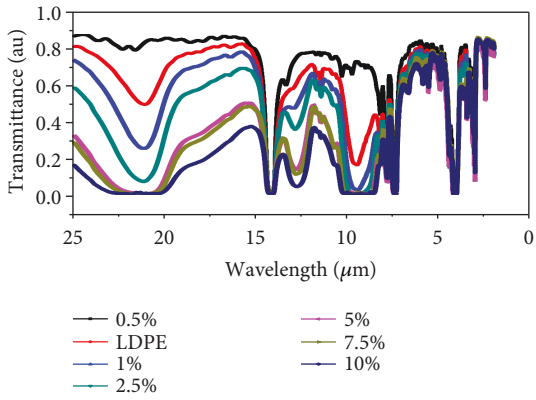

Figure 5: FTIR spectra for different ratios of LDPE/silica nanocomposite films.

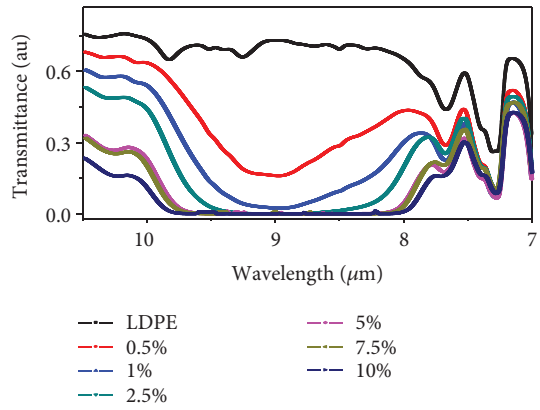

Figure 6: FTIR spectra in the range 7-10.5 μm.

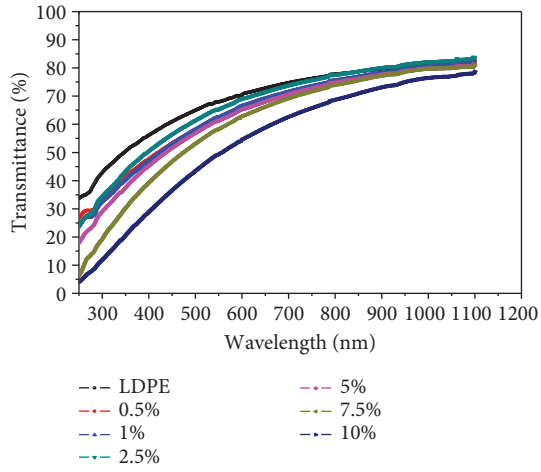

Figure 7: UV-visible spectra of LDPE/silica nanocomposite films.

SiO_2 its importance and allows it to be used in this application. We observe a decrease in the transmittance when the mixing ratio of SiO_2 increases. The changes in the average transmittance for wavelengths ranging from 7 to 10.5 μm are shown in Figure 6. We notice a sharp decline in transmittance when the ratio of SiO_2 is increased.

3.2.2. Ultraviolet-Visible Spectroscopy Study. The optical transmittance measurements of LDPE/silica nanocomposite substrate films were carried out with a UV-Vis-NIR spectrophotometer (A560 UV Spectrophotometer, AOE Instruments) at the normal incident of light in the wavelength range of 200-1100 nm. Figure 7 shows the transmittance spectra of the samples. The UV spectra show that the composite substrates (0.5, 1, 2.5, 5, and 7.5 wt% SiO_2) have no significant effect on the transmittance. On the other hand, a significant decrease in the transmittance is observed with a mixture ratio of 10 wt% SiO_2 compared to the LDPE without mixing. This decrease is addressed in Results and Discussion.

3.3. Thermal Study. We built a minigreenhouse using LDPE without mixing and another one using LDPE mixed with 2.5 wt% SiO_2. We also built a third minigreenhouse using window silka glass (the glass thickness is 6 mm, and the transmittance from 350 to 1100 nm is approximately 88%) (see Figure 8). All the three greenhouses have a cube shape with sides measuring 20 cm. Inside each greenhouse, we put a small plant. These plants were previously grown under similar conditions.

The temperature inside each greenhouse was measured using identical temperature sensors (Tecnologic UK with 0.1°C resolution). The external temperature was also measured using an identical sensor. All the measurements were made at the same moment every thirty minutes starting from 1 p.m. until 6 a.m. the next day. Figure 9 shows the temperature variations inside the three greenhouses along with the external air temperature. An increase in the temperature inside the greenhouse mixed with 2.5 wt% SiO_2 is noticed. This increase is estimated to be more than 2°C compared with the LDPE greenhouse without mixing (2°C overall and 2.2°C between 11 PM and 5 AM). We also notice that the transmittance of the greenhouse mixed with 2.5 wt% SiO_2 closely approaches that of the glass house (see the green and blue triangles in Figure 9). In fact, the average temperature difference is about 0.14°C overall and the two temperatures between 11 PM and 5 AM match each other very well.

(a) (b)

(c)

Figure 8: Three greenhouses: (a) LDPE without mixing, (b) LDPE mixed with 2.5 wt% SiO_2, and (c) silica glass. This figure was reproduced from Alghdeir et al. [9] (under the Creative Commons Attribution License/public domain).

By studying the IR transmission in Figures 5, 6, and 10, a decrease in the transmittance near 9 μm with increasing mixture ratios is noticed. This result explains the rise in temperature inside the minigreenhouses (shown in Figure 10). The LDPE/silica nanocomposite barrier films preserve the thermal radiation of the ground. Thus, the internal temperature inside the greenhouse is maintained.

One can also notice that in the vicinity of 9 μm, the transmittance of the sample with a ratio of 5 wt% SiO_2 is very close to that of the sample with a ratio of 2.5 wt% SiO_2. We deduce that it may not be very beneficial to go beyond a ratio of 2.5 wt% SiO_2.

By studying the UV-VIS transmission in Figure 7, a significant decrease is noticed in the transmittance of the film with a ratio of 10 wt% SiO_2, compared with the other films with a lesser ratio (0.5, 1, 2.5, 5, and 7.5 wt% SiO_2). These five composite barrier films do not have any significant effect on the transmittance compared with that of the LDPE without

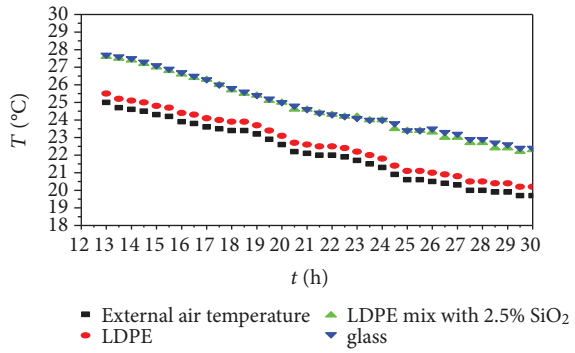

Figure 9: The variations of the difference of temperature (ΔT) between the temperature inside the greenhouse and the temperature in the external air during the time.

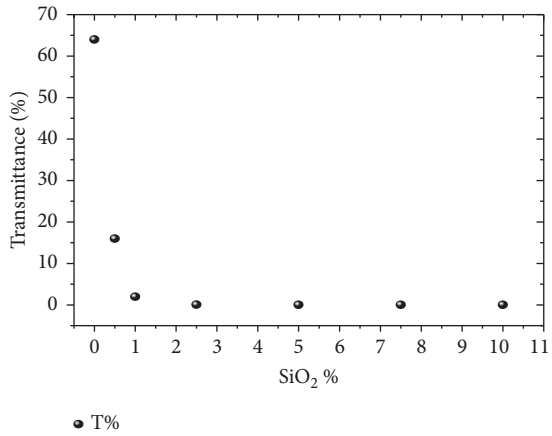

Figure 10: Transmittance at 9 μm as a function of different ratios of SiO_2.

mixing. Thus, the film with a ratio of 2.5 wt% SiO_2 composite was adopted to build the minigreenhouse. It has no effect on the UV-VIS transmission but it reduces the maximum transmission of the IR radiation to around 9 μm.

The refractive index of LDPE in the visible domain is 1.51, while the imaginary part is $k = 0$ [15]. It is very close to the value of the real part of the refractive index of SiO_2 which is equal to 1.43 [16]. Therefore, there should not be any significant change in the transmittance of the LDPE in the visible range when mixed with SiO_2. This is clearly seen in Figure 7) except for the last case where the ratio of SiO_2 is 10 wt%. Consequently, there should not be any significant change in the greenhouse temperature during sun-shining time. The significant reduction in the transmittance in the case where the ratio of 10 wt% SiO_2 is probably due to Mie scattering [17].

4. Conclusion

Throughout this study, silicon dioxide films with different ratios (0.5, 1, 2.5, 5, 7.5, and 10 wt% SiO_2) were mixed with a low-density polyethylene (LDPE) polymer using the melt mixing technique.

The effect of the incorporation of 0.5–10 wt% of silica particles to a tensile property of LDPE was investigated. The results showed that the addition of 1 wt% of nanosilica has successfully enhanced the tensile strength and elongation at break of the nanosilica-filled LDPE material. The incorporation of >1 wt% of nanosilica particles had caused agglomeration and uneven distribution of the particles in LDPE.

By using these LDPE/silica nanocomposites to build a minigreenhouse, SiO_2 reduces the transmission of radiation near 9 μm and allows the transmission of ultraviolet and visible radiation to pass through them during daytime (period of sunshine, without being exposed to direct sunshine). Thus, we were able to preserve the thermal radiation of the ground by raising the internal temperature of the greenhouse up to more than 2°C, compared with the same greenhouse without mixing. The temperature inside the LDPE/silica greenhouse was found to be almost identical to that inside the glass greenhouse.

Statistically speaking, the conclusions are acceptable because the experiment was replicated many times. The main gain is the fact that the LDPE/silica greenhouse has the same temperature as the glass-made greenhouse.

Data Availability

The data used to support the findings of this study are available from the corresponding author upon request.

Conflicts of Interest

The authors declare that they have no conflicts of interest.

References

[1] A. Kuzminova, A. Shelemin, M. Petr, O. Kylian, and H. Biederman, "Barrier coatings on polymeric foils for food packaging," in *WDS'13 Proceedings of Contributed Papers, Part III*, pp. 128–133, Prague, Czech Republic, 2013.

[2] O. Kylián, A. Choukourov, L. Hanyková, and H. Biederman, "Plasma technology for polymer food packaging materials," in *Ecosustainable Polymer Nanomaterials for Food Packaging: Innovative Solutions, Characterization Needs, Safety and Environmental Issues*, p. 119, Taylor and Francis Group, 2013.

[3] S. Ju, M. Chen, H. Zhang, and Z. Zhang, "Dielectric properties of nanosilica/low-density polyethylene composites: the surface chemistry of nanoparticles and deep traps induced by nanoparticles," *Express Polymer Letters*, vol. 8, no. 9, pp. 682–691, 2014.

[4] H. H. Redhwi, M. N. Siddiqui, A. L. Andrady, and S. Hussain, "Durability of LDPE nanocomposites with clay, silica, and zinc oxide: part I: mechanical properties of the nanocomposite materials," *Journal of Nanomaterials*, vol. 2013, Article ID 654716, 6 pages, 2013.

[5] A. Pal, *Low-Power VLSI Circuits and Systems*, Springer India, 2015.

[6] A. Yasunas, D. Kotov, V. Shiripov, and U. Radzionay, "Low-temperature deposition of silicon dioxide films in high-density plasma," *Semiconductor Physics, Quantum Electronics & Optoelectronics*, vol. 16, no. 2, pp. 216–219, 2013.

[7] A. Delimi, Y. Coffinier, B. Talhi, R. Boukherroub, and S. Szunerits, "Investigation of the corrosion protection of SiOx-like oxide films deposited by plasma-enhanced chemical vapor deposition onto carbon steel," *Electrochimica Acta*, vol. 55, no. 28, pp. 8921–8927, 2010.

[8] W. T. Li, R. Boswell, M. Samoc, A. Samoc, and R. P. Wang, *Thin Solid Films*, vol. 516, no. 16, pp. 5474–5477, 2008.

[9] M. Alghdeir, K. Mayya, M. Dib, and I. Alghoraibi, "Characterization of SiO_2/LDPE composite barrier films," *Journal of Materials and Environmental Sciences*, vol. 9, no. 7, pp. 2042–2050, 2018.

[10] Z. Liu, Z. Sun, X. Ma, and C. L. Yang, "Characterization of composite SiOx/polymer barrier films," *Packaging Technology and Science*, vol. 26, pp. 70–79, 2013.

[11] J. Lange and Y. Wyser, "Recent innovations in barrier technologies for plastic packaging—a review," *Packaging Technology and Science*, vol. 16, no. 4, pp. 149–158, 2003.

[12] H. Zou, S. Wu, and J. Shen, "Polymer/silica nanocomposites: preparation, characterization, properties, and applications," *Chemical Reviews*, vol. 108, no. 9, pp. 3893–3957, 2008.

[13] C. Y. Chee, N. L. Song, L. C. Abdullah, T. S. Y. Choong, A. Ibrahim, and T. R. Chantara, "Characterization of mechanical properties: low-density polyethylene nanocomposite using nanoalumina particle as filler," *Journal of Nanomaterials*, vol. 2012, Article ID 215978, 6 pages, 2012.

[14] R. Kitamura, L. Pilon, and M. Jonasz, "Optical constants of silica glass from extreme ultraviolet to far infrared at near room temperature," *Applied Optics*, vol. 46, no. 33, pp. 8118–8133, 2007.

[15] B. S. Mitchell, *An Introduction to Materials Engineering and Science for Chemical and Materials Engineers*, John Wiley & Sons, 2004.

[16] C. Xiong, W. Xu, Y. Zhao, J. Xiao, and X. Zhu, "New design graded refractive index antireflection coatings for silicon solar cells," *Modern Physics Letters B*, vol. 31, no. 19-21, article 1740028, 2017.

[17] M. Iqbal, *An Introduction to Solar Radiation*, Elsevier, 2012.